Magnetic behavior of $PrNi_2B_2C$ single crystals

A. Durán,[1] S. Bernès,[2] and R. Escudero[1]
[1]*Instituto de Investigaciones en Materiales, Universidad Nacional Autónoma de México, Apartado Postal 70-360, México D.F., 04510, Mexico*
[2]*Centro de Química, ICUAP, AP 1613, Puebla Pue., Mexico*
(Received 27 August 2001; revised manuscript received 4 April 2002; published 31 December 2002)

We have studied the magnetic and transport properties of $PrNi_2B_2C$ single crystals. Magnetic measurements at low field show the presence of a magnetic ordering in $\chi(T)$ curves at 15 K. M-H isotherms from 15 to 2 K show hysteresis in *ab* and *c* crystallographic directions. Below 4 K the ground state looks like a ferromagnetic state. Resistivity measurements in the *a*-*b* plane, $\rho_{a\text{-}b}$, indicate metallic behavior down to 300 mK but without traces of superconductivity. The magnetism at 15 K seems to be the main reason for the absence of superconductivity in this material.

DOI: 10.1103/PhysRevB.66.212510 PACS number(s): 74.70.Dd, 74.25.Ha

$PrNi_2B_2C$ (Pr221) is an interesting member of the borocarbide family. It shows a moderated heavy fermion behavior, is not superconducting, and displays many different magnetic characteristics at low temperatures. In general, interest in borocarbide materials has been directed to the study of the competition between magnetism and superconductivity.[1–5] The type of interaction in these systems with rare earth and transition metals is the complex effect between *f* electrons and the *d*-conduction band, which play important roles in the electronic properties. The main consequence is that the rare earth moments polarize the conduction electrons via the exchange mechanism known as the Ruderman-Kittel-Kasuya-Yosida (RKKY) interaction, hybridizing the two electronic populations: the *f* electrons and the *d*-conduction band. The result of these processes is that the magnetic properties have a great influence on the electronic transport in these materials.

Systems with RNi_2B_2C (R221), where $R=$ Pr, Nd, Gd, and Tb, show magnetism, but not superconductivity. In these compounds the antiferromagnetic (AFM) ordering is found at temperatures from 4 K for Pr221 (in polycrystalline samples), 15 K for Tb221, to 20 K for Gd221.[6,7] If one follows the trend of the Ni-Ni distance and the de Gennes factor through the members of the family,[8,9] one would expect that Pr221 would be superconducting at a temperature of about 3.5 K. However, superconductivity has not been observed in these materials in measurements down to 300 mK.[10] In order to have a better understanding of the electronic nature of this system, further measurements of the transport and magnetic properties on single crystals are needed. In this work we report magnetic and transport studies performed on high quality Pr221 single crystals. The most important finding is the magnetic ordering at about 15 K, which persists below 4 K, and that we think is related with the absence of superconductivity in this compound.

The single crystals were grown using a water-cooled copper crucible in a radio-frequency induction furnace.[10] The purities of the starting materials were Pr 99.9%, Ni 99.99%, B 99.8%, and C 99.9998%. Single crystals were studied at room temperature by x-ray diffraction (Bruker P4 diffractometer, graphite monochromatized Mo-Kα radiation). A long-time exposure photographic experiment was unable to detect secondary phases such as $PrNi_3$ and PrNi, which show ferromagnetic order at about 20 and 22 K, respectively.[11] On the other hand, observed diffraction peaks are symmetrical, with low background, over a complete diffraction sphere up to 0.50-Å resolution. The set of spots indexed yield the expected cell parameters $a=3.696(1)$ Å and $c=10.033(1)$ Å. Finally, the fullwidth at half maximum for strong reflections, estimated as 0.32(1) (a block size of circa, 150 Å in the Scherrer approximation), together with the high value of the empirical extinction parameter obtained during the refinement of the structure, $x=0.067(6)$.[12] Hence we exclude the possibility of microscopic polycrystalline aggregates. On the basis of these data, we estimate that the single crystals under consideration here are pure crystalline samples of Pr221.

Magnetization measurements were obtained using a Quantum Design superconducting quantum interference device magnetometer with the magnetic field applied along the *a*-*b* plane and the *c* direction of the platelet-like single crystals. The $M(H,T)$ data were taken in zero field cooling (ZFC) and field cooling (FC) modes. The isothermal loops were measured with a maximum magnetic field from zero to ± 50 kOe. The resistivity measurements were made in single crystals with typical dimensions of about $2.5\times3\times0.5$ mm^3. In this case the measurements were performed from 2 to 300 K using four 25-μm gold wires attached with silver paint, and the applied dc current flowing in the *a*-*b* plane. The crystals show a metallic behavior from 300 to $\sim$10 K, with a resistivity ratio $\rho_{a-b(300K)}/\rho_{a-b(1.8K)}$ of 10.5.

Figure 1 shows representative data of the susceptibility versus temperature from 24 to 2 K in the presence of low magnetic field (10 Oe) measured in the FC mode, in both directions of the crystal. The anomaly at about 15 K marks the onset of the spontaneous magnetization which seem indicated a ferromagnetic transition, as will be discussed below. From 15 to about 8 K the curve shows a steep increase of the magnetization. At about 8 K a dramatic change is observed in the slope of the curves, this being most clearly defined in the *a*-*b* plane. At about 2 K the $\chi(T)$ curves of both directions show a change of slope characterized by a slightly plateau, being more pronounced along the *a*-*b* plane. The inset in Fig. 1 shows the susceptibility data ($\chi-T$) measured in the ZFC mode, along with $\rho(\mathbf{T})$ over the same tem-

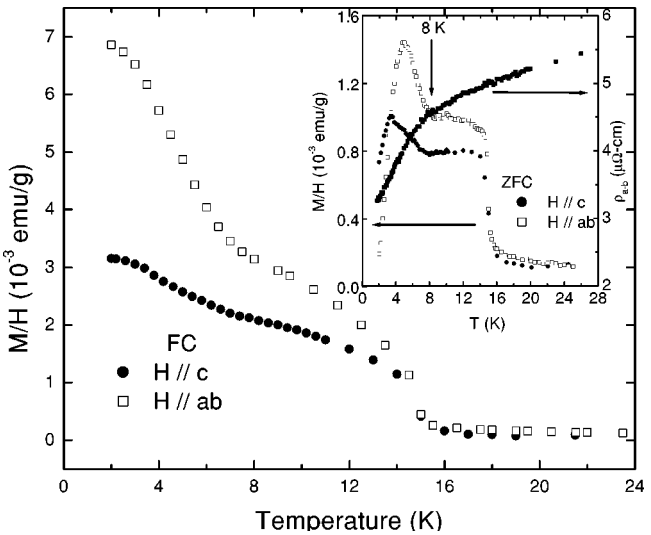

FIG. 1. Susceptibility vs temperature ($\chi - T$) for a $PrNi_2B_2C$ single crystal with applied magnetic field (10 Oe) in the *a*-*b* plane and *c* direction, from 25 to 2 K in the FC mode. The inset shows susceptibility data in the ZFC mode. The inset also shows the temperature dependence of the electrical resistivity in the *a*-*b* plane from 1.8 to 25 K.

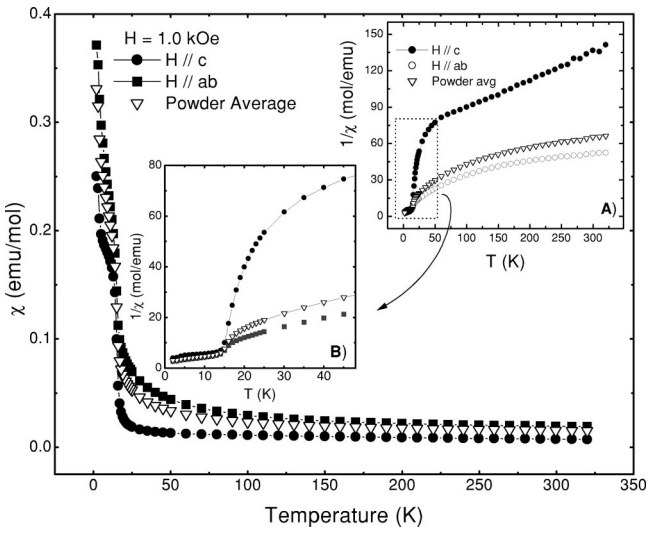

FIG. 2. The anisotropy of the susceptibility curves from 2 to 310 K with an applied field of 1 kOe, for the *a*-*b* plane, the *c* direction, and the powder average. The insets shows (A) $1/\chi$ vs T obtained from the susceptibility data from 2 to 310 K. (B) The low temperature $1/\chi$ vs T data in an expanded scale.

perature region. Firstly a steep increase in the $\chi(T)$ curve at about 15 K is observed, and below 8 K an inflection appears in both directions. The curves have maxima at about 3.5 and 4.8 K in the *a*-*b* plane and the *c* parallel direction, respectively. It is related to the AFM transition previously observed by Lynn *et al.*[6] In the same inset we show that, in the resistivity versus temperature measurements, there is a sharp decrease of $\rho(T)$ at about 8 K. This is associated with a decreasing of magnetic scattering due to the long range antiferromagnetic order which is completed at about 4 K, in a similar way as was observed in a Ho221 system with neutron measurements.[6,13] We can estimate the exchange interaction strength (I_{ex}) for this compound taking the resistivity drop between 8 and 1.8 K ($\Delta\rho = 0.94\ \mu\Omega - \mathrm{cm}$) to be $I_{ex} = 9.23$ meV, which is much higher than the values previously reported for other rare earth compounds, i.e., Dy (3.99 meV), Tb (5.2 meV), and Ho (5.06 meV).[15,16] It is reasonable to expect a high value of I_{ex} compared with other members of this family. For instance, diffraction analysis shows that the lattice parameter *c* decreases by about 5.2% from Ho221 to Pr221. This contraction is a consequence of the enlargement of the Ni-Ni interatomic distance from 2.4826(1) Å for Ho221 to 2.6160(1) Å for Pr221. The substantial contraction of the *c* axis clearly indicates a strong interplane exchange mediated by Ni-B layers which implies an enhancement of I_{ex}.

Figure 2 shows the $\chi(T)$ measured in a magnetic field of 1 kOe, from 310 to 2 K. The measurements were taken in both directions of the crystal. At low temperature, $\chi(T)$ is larger for the $H \perp c$ direction than the $H \| c$ direction. From these data we can infer that the easy spins orientation are in the basal plane of the tetragonal structure, as has been suggested by neutron diffraction measurements on polycrystalline samples.[6] Inset (A) in Fig. 2 shows $1/\chi(T)$ in the two directions of the crystal, and the calculated powder average. At 15 K we observed a dramatic change of linearity in the curves. This onset may be characterized very well as a ferrimagnetic transition; however, we cannot rule out this as ferromagnetism. Using a fit with the Curie-Weiss law from 100 to 310 K, we found that the effective moment (μ_{eff}) for the Pr ion is about $(3.465 \pm 0.004)\mu_B$, $(2.380 \pm 0.013)\mu_B$, and $(3.142 \pm 0.007)\mu_B$ for $H \perp c$, $H \| c$, and the powder average, respectively. The values for $H \perp c$, and the powder average are slightly lower than the theoretical value of $\mu_{eff} = 3.56\mu_B$ for the isolated Pr^{+3} ion. Furthermore, we observe that the magnetic moment decreased by $1.3\mu_B$ in the *c* direction. This indirect evidence suggests that Pr may be in an intermediate valence state, because the effective moment in

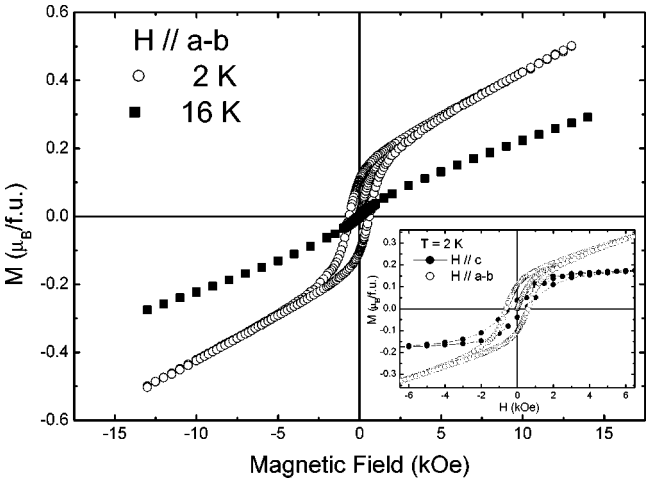

FIG. 3. The magnetization versus applied magnetic field in the *a*-*b* plane at 2 and 16 K. The inset shows the anisotropic behavior of the magnetization at $T = 2$ K in the *a*-*b* plane and the *c* direction of the single crystal.

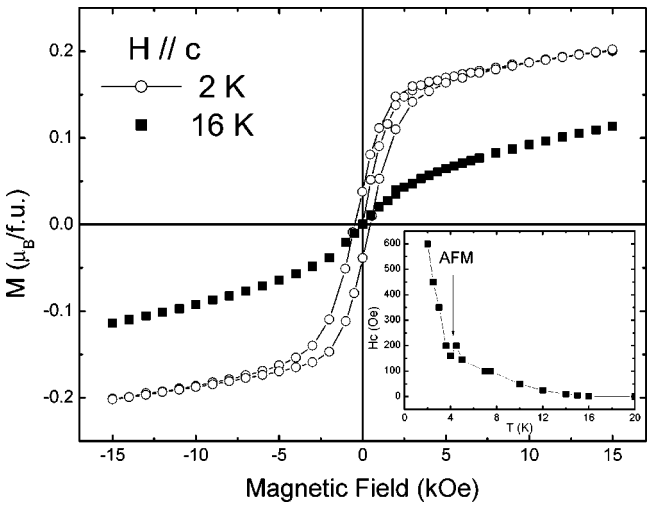

FIG. 4. The magnetization vs the applied magnetic field in the *c* direction at 2 and 16 K. The inset shows the coercive force as a function of temperature.

the *c* direction is close to the expected for Pr^{+4} ($2.54\mu_B$). Inset (B) shows an expanded plot of the data below 50 K; this figure shows a typical ferrimagnetic hyperbolic drop instead of ferromagnetic behavior. The negative extrapolated Weiss temperature (θ_w) is in clear contrast with positive values for a ferromagnet. Temperature- and field-dependent specific heat measurements were recently been completed by our group.[14] These measurements show a sharp jump in $Cp(T)$ at 15 K. The sharpness and amplitude are reduced with increasing magnetic field in a similar way as that observed in the derivative magnetization data (inset of Fig. 5). However, temperature dependent neutron scattering measurements in single crystals will help to understand the true nature of the magnetic transition at 15 K.

Figures 3 and 4 show the *M*-*H* data in terms of μ_B per unit formula (f.u.) for the applied magnetic field along the *a*-*b* plane and the *c* direction at two temperatures, 2 and 16 K. The hysteresis measured at 2 K confirms the existence of magnetic ordering in both directions. The coercive field measured is about 610 Oe, for both directions. The measurements of the *M*-*H* curves show that the hysteresis disappears at about 15 K. In the inset of Fig. 3 we show the anisotropy hysteresis at 2 K in both directions of the crystal. More extensive information on the behavior of the coercive data, $H_c(T)$, can be seen in the inset of Fig. 4. The coercivity begins to appear at 15 K and increases as the temperature decreases, the arrow marks the AFM transition in the H_c vs T curve. Another feature is that the magnetic order which start at 15 K is stronger than the weak ferromagnetism (WFM) observed in other compounds of this borocarbide family. For instance, in Er221 WFM takes place at 2.5 K, and coexists with superconductivity, while in Tb221 it occurs at 6 K.[15,17]

Figure 5 shows the *M*-*T* curves taken at different magnetic fields applied along the *a*-*b* plane and the *c* direction at 2 K. For a magnetic field of about 50 kOe, the saturation value increases to $\sim 2.7\mu_B$/f.u., in the *a*-*b* plane whereas about $1.4\mu_B$/f.u. is reached in the *c* direction. As we can see, the saturation paramagnetic moment of Pr221 is below that

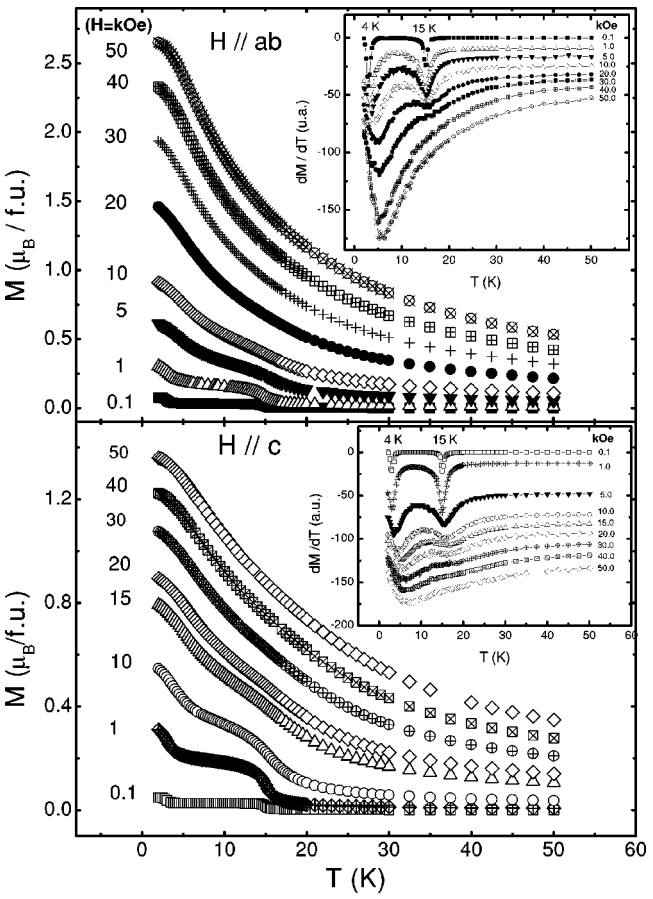

FIG. 5. The magnetization vs temperature (*M*-*T*) for several magnetic fields in the *a*-*b* plane and the *c* direction. The inset shows dM/dT as a function of temperature. Two anomalies at 15 and 4 K are indicated.

of the theoretical maximum magnetization ($3.56\mu_B$/f.u.) and this behavior is quite different from that as *R*221, with *R* = Tb, Er, Dy, and Ho, which shows a saturated magnetization close to the theoretical maximum magnetization value.[4,15,18,19] It is also interesting to note in this figure that the two magnetic transitions at 15 and 4 K are readily seen at low magnetic fields but tend to vanish when the field is increased. In order to see more clear this behavior the insets show dM/dT as a function of temperature. At low fields, there are two sharp peaks at 4 and 15 K, corresponding to AFM according to Lynn *et al.*[6] and to weak magnetic ordering, respectively. It is important to mention that WFM occurs where AFM ordering is incomplete. The opposite moments are not quite collinear and while they almost cancel a small spontaneous magnetization exist. AF can also result of helical ordering of the magnetic moments and spontaneous magnetization can appear in the system. As the magnetic field increases the magnetic transition at 15 K disappears at approximately 15 kOe. This behavior can be explained according to Dzyaloshinsky-Moriya interaction, as also used by Cho *et al.*[15] to elucidate the relation between the easy magnetization direction and the occurrence of WFM in Tb221. They suggested two different canted AFM states, which can be stable in the [100] or [110] directions of the tetragonal

structure for a magnetic field applied perpendicular to the *c* direction. Based on this, we also speculate that Pr221 presents canted moments that can be stabilized along the easy magnetization direction [110]. This direction has been determined as the easy magnetization direction in Dy221, Ho221, and Pr221 by neutron diffraction measurements.[6,20,21] Under this scenario, we suppose that these canted spins rotate under the influence of the magnetic field and are probably destabilized above 15 kOe. This might explain the vanishing of the magnetic transition, as we can see in the derivative magnetization dM/dT in the insets of Fig. 5. Another remarkable feature in the insets is the shift of the peaks at 4 K toward higher temperatures when the magnetic field is increased. This striking feature of the Pr221 compound has not been observed in the homologue Tb221, Er221, and Ho221 single crystals. In these compounds, the AFM transition is shifted toward lower temperatures, the transition disappears, and the magnetization saturates at higher magnetic fields.[5,15,22]

In summary, magnetic and transport measurements show that $PrNi_2B_2C$ single crystals present two magnetic transition at ~ 15 and ~ 4 K. The magnetic transition at 15 K seems to arise from two interpenetrated structures formed by Pr^{+3} ions, one of which has a canted spin. The magnetization is higher in the *a*-*b* plane, which shows that the easy magnetization is on this plane. Finally, no traces of superconductivity were detected by magnetization and resistivity measurements. The lack of superconductivity may be associated with the existence of the magnetic ordering below 15 K. However, neutron scattering measurements will be necessary in single crystals in order to understand in more detail the magnetic transition at 15 and 4 K in $PrNi_2B_2C$.

A.D. and R.E. thank CONACyT and UNAM-DGAPA through Project No. G-0017, and 1N-105597. We thank J. Guzmán for the WDX/EDX analysis and Dr. S. Muhl for a critical reading of the manuscript.

[1] R. Nagarajan, C. Mazumdar, Z. Hossain, S.K. Dhar, K.V. Gopalakrishnan, L.C. Gupta, C. Godart, B.D. Padalia, and R. Vijayaraghavan, Phys. Rev. Lett. **72**, 274 (1994).

[2] R.J. Cava, H. Takagi, H.W. Zandbergen, J.J. Krajewski, W.F. Peck, Jr., T. Siegrist, B. Batlogg, R.B. Van Dover, R.J. Felder, K. Mizahuashi, J.O. Lee, H. Eisaki, and S. Uchida, Nature (London) **367**, 2521 (1994).

[3] H. Eisaki, H. Takagi, R.J. Cava, B. Batlogg, J.J. Krajewski, W.F. Peck, K. Mizuhashi, J.O. Lee, and S. Uchida, Phys. Rev. B **50**, 647 (1994).

[4] P.C. Canfield, B.K. Cho, D.C. Johnston, D.K. Finnemore, and M.F. Hundley, Physica C **230**, 397 (1994).

[5] B. K. Cho, P. C. Canfield, L. L. Miller, D. C. Johnston, W. P. Beyermann, and A. Yatskar, Phys. Rev. B **52**, 3684 (1995).

[6] J.W. Lynn, S. Skanthakumar, Q. Huang, S.K. Sinha, Z. Hossain, L.C. Gupta, R. Nagarajan, and C. Godart, Phys. Rev. B **55**, 6584 (1997).

[7] P.C. Canfield, B.K. Cho, and K.W. Dennis, Physica B **215**, 337 (1995).

[8] C.C. Lai, M.S. Lin, Y.B. You, and H.C. Ku, Phys. Rev. B **51**, 420 (1995).

[9] V.N. Narozhnyi, J. Freudenberger, G. Fuchs, K. Nenkov, D. Eckert, A. Czopnik, and H.K. Muller, J. Low Temp. Phys. **117**, 1599 (1999).

[10] A. Durán, E. Muñoz, S. Bernès, and R. Escudero, J. Phys.: Condens. Matter **12**, 1 (2000).

[11] Y. Y. Pan and P. Nash, in *Phase Diagrams of Binary Nickel Alloys*, edited by P. Nash (ASM International, 1991), Series 6, p. 256.

[12] The empirical formula used in SHELX97 covers both primary and secondary extinction. See G.M. Sheldrick, SHELX97 Users Manual, University of Göttingen, Germany, Ch. **7** (1997).

[13] J.W. Lynn, Q. Huang, A. Santoro, R.J. Cava, J.J. Krajewski, and W.F. Peng, Jr., Phys. Rev. B **53**, 802 (1996).

[14] F. Morales, A. Durán, and R. Escudero (unpublished).

[15] B.K. Cho, P.C. Canfield, and D.C. Johnston, Phys. Rev. B **53**, 8499 (1996).

[16] A.K. Bhatnagar, K.D.D. Rathnayaka, D.G. Naugle, and P.C. Canfield, Phys. Rev. B **56**, 437 (1997).

[17] P.L. Gammel, B. Barber, D. Lopez, A.P. Ramirez, D.J. Bishop, S.L. Budko, and P.C. Canfield, Phys. Rev. Lett. **84**, 2497 (2000).

[18] R. Szymczak, M. Baran, L. Gladczuk, H. Szymzack, Z. Drzazga, and A. Winiarska, Physica C **254**, 124 (1995).

[19] P.C. Canfield and S.L. Budko, J. Alloys Compd. **262-263**, 169 (1997).

[20] B.K. Cho, B.N. Harmon, D.C. Johnston, and P.C. Canfield, Phys. Rev. B **53**, 2217 (1996).

[21] C. Sierks, M. Doerr, A. Kreyssing, M. Loewenhaupt, Z.Q. Peng, and K. Winzer, J. Magn. Magn. Mater. **192**, 473 (1999).

[22] K.D.D. Rathnayaka, D.G. Naugle, B K. Cho, and P.C. Canfield, Phys. Rev. B **53**, 5688 (1996).